



Experimental and theoretical investigation into the elimination of organic pollutants from solution by layered double hydroxides

Xin Liu, Xiaofei Zhao, Yue Zhu, Fazhi Zhang*

State Key Laboratory of Chemical Resource Engineering, Beijing University of Chemical Technology, Beijing 100029, China



ARTICLE INFO

Article history:

Received 8 November 2012
Received in revised form 26 March 2013
Accepted 1 April 2013
Available online 11 April 2013

Keywords:

Layered double hydroxides
Organic pollutants
Photoassisted
Density functional theory

ABSTRACT

This work aims at revealing the role of pristine layered double hydroxide (LDH) materials in the elimination of organic pollutants from solution. Typical LDH samples, ZnCr- and MgAl-LDHs (with Zn^{2+}/Cr^{3+} or Mg^{2+}/Al^{3+} molar ratio 2), are prepared and used for the removal of methylene blue (MB), methyl orange (MO), and formaldehyde. The systematic investigations of structural characterization and periodic density functional theory (DFT) calculation of the LDH samples demonstrate that: (1) no electron–hole pairs could be generated for MgAl-LDHs under the irradiation of visible light due to the large calculated gap energy above 5.0 eV. (2) ZnCr-LDHs are sensitive to the irradiation of visible light with the calculated gap energy between 2.0 and 3.0 eV, but the rapid charge recombination and low efficiency in electron/hole separation would suggest that photocatalytic activity of ZnCr-LDHs would be greatly limited. In the experimental work, ZnCr- and MgAl-LDHs show no photocatalytic activity for the removal of formaldehyde under the visible light. The disposal of the organic dyes molecules in the solution would be caused by the photoassisted degradation and surface adsorption effect rather than the photocatalysis impact for both LDH samples. This is confirmed by the elimination tests that carry out in the dark condition with the similar procedure under visible light irradiation. Moreover, the two types of LDH samples exhibit the different adsorption capability for the MB and MO molecules due to the different colloidal properties of the LDH samples, which is revealed by Zeta potential measurement. The above finding that elimination of organic dyes from solution by the pristine LDH samples through photoassisted degradation and adsorption processes would be important for the rational design and use of clay-like materials for the treatment of sewage containing toxic compounds.

© 2013 Elsevier B.V. All rights reserved.

1. Introduction

Over the past few decades, there have been increasing demands for solutions to the multiple environmental problems associated with sewage containing toxic compounds. Organic pollutants have been extensively used with high toxicity and hard-degradation. Therefore, many efforts have been made to developing methods for the elimination of such organic compounds from wastewater by means of biological and physical-chemical techniques [1]. One important branch refers to the development of suitable adsorbents used in the elimination of organic pollutants, including activated carbons [2], zeolites [3], and layered double hydroxide (LDH)-derived materials [4]. LDH is a family of two-dimensional anionic clays with the general formula $[M^{2+}_{1-x}M^{3+}_x(OH)_2]A^{n-}_{x/n}\cdot mH_2O$, where M^{2+} and M^{3+} are di- and trivalent cations, respectively; the value of the coefficient x is equal to the molar ratio of $M^{3+}/(M^{2+} + M^{3+})$; and A^{n-} is an anion [5–9]. LDH and their

calcination products have been successfully employed as adsorbent materials for a variety of anion species and/or pollutants, including sulfur oxides [10], sodium dodecylsulfate [11], synthetic dyes [12], and pesticides [13–15]. Based on the structure and intercalation characters of LDH, there are three kinds of uptake mechanisms presented: surface adsorption, interlayer anion exchange, and reconstruction of calcined LDH by the “memory effect” [16].

Another effective strategy for the elimination of organic pollutants from wastewater is the photocatalytic performance of semiconductor materials such as TiO_2 [17–19], ZnO [20–23], and CdS [24–26] have been intensively investigated. All these semiconductors could act as sensitizers for light-reduced redox processes due to their electronic structure, which is characterized by a filled valence band (VB) and an empty conduction band (CB) [27,28]. When a photon with energy of $h\nu$ matches or exceeds the band gap energy, E_g , of the semiconductor, the electrons transferred from the VB to the CB and generated the photogenerated charge carriers, i.e., electrons (e^-) and holes (h^+) pairs, which are powerful reductants and oxidants, respectively. Considering the di- and trivalent metal ions on the main layers of LDH could

* Corresponding author. Fax: +86 10 64425385.

E-mail address: zhangfz@mail.buct.edu.cn (F. Zhang).

be varied in a wide range without altering the structure [29]. LDH would be envisioned as providing the opportunity of having doped semiconductors or semiconductor composite materials after thermal treatment at high temperature and such semiconductor composites could be served as excellent photocatalytic materials [30–32]. Some investigations about the elimination of organic dyes from wastewater over LDH-related materials believe that LDH could be regarded as semiconductor materials and photocatalytic degradation processes may take place. For instance, Mantilla et al. [33] investigated the photocatalytic properties of series of ZnAlFe-LDHs materials. It was revealed that, after the reconstruction of LDH by calcination/rehydration processes, the activated ZnAlFe-LDHs could play the role of photocatalyst for the degradation of 2,4-dichloropenoxyacetic. They pointed out that Fe^{3+} ions in the ZnAlFe-LDHs provoke important variations in the semiconductor properties of the materials which accounted for the photocatalytic activity. They also reported the photoassisted activities of MgAl-LDHs, and this activity was explained by a photo excitation which produced mobility charges in the lamellar structure of MgAl-LDHs [34]. Shao et al. demonstrated the applications of ZnTi-LDHs displayed superior photocatalytic activity in the visible light for decomposition of MB [35], but the MB might be not suit for photocatalytic activity test, since the photoinduced reaction by MB photoadsorption would mislead into believing that a given semiconductor material has visible-light photocatalytic activity [36]. On the other hand, the investigations about series of MgZnAl-LDHs demonstrated that [37] the large band gap values of such materials indicated a diminished semiconducting capacity, but they still exhibited photocatalytic activity for the degradation of pollutants. The authors also suggested that the residual small amount of ZnO after the reconstruction of MgZnAl-LDHs led to the photocatalytic activity. Moreover, the higher specific surface area presented by the materials could not be overlooked. Although Silva et al. proposed that ZnCr-LDHs could be used as excellent photocatalyst for oxygen generation from splitting of water under visible light irritation, special sacrificial acceptor solution (i.e., AgNO_3) was necessary [38]. Naturally, one question comes to us: whether the removal pathways of pollutant molecules are carried out over LDH materials through intrinsic photocatalytic processes as a result of the textual characters of LDH?

Herein, in order to disclose the reason for the above question, two typical pristine LDH samples, ZnCr-LDHs (which is viewed as semiconductor (mixed oxides) and exhibited adsorption peaks in the visible region [38,39]), and MgAl-LDHs (which is not considered to be capable of generating the e^- and h^+ pairs by band gap under visible light irradiation [34,37]) are prepared and applied for the elimination of different pollutants, methylene blue (MB), methyl orange (MO), and formaldehyde with or without irradiation of visible light. The periodic density functional theory (DFT) calculations which have been applied in the photocatalyst design and analysis [40,41] is also performed to predict the electronic band structure of ZnCr- and MgAl-LDHs. The structural and optical properties of both LDH samples are characterized by powder X-ray diffraction (XRD), room temperature Fourier transform infrared spectra (FT-IR), N_2 sorption measurements, and ultraviolet-visible spectra (UV-vis). The elimination results are carefully discussed and compared with the DFT calculation results of LDH samples.

2. Experimental

2.1. Models and computational methods

The parent LDH material is the naturally occurring mineral MgAl-LDHs whose microstructure with $\text{Mg}^{2+}/\text{Al}^{3+}$ ratio of two or three has been studied by using quantum chemistry methods

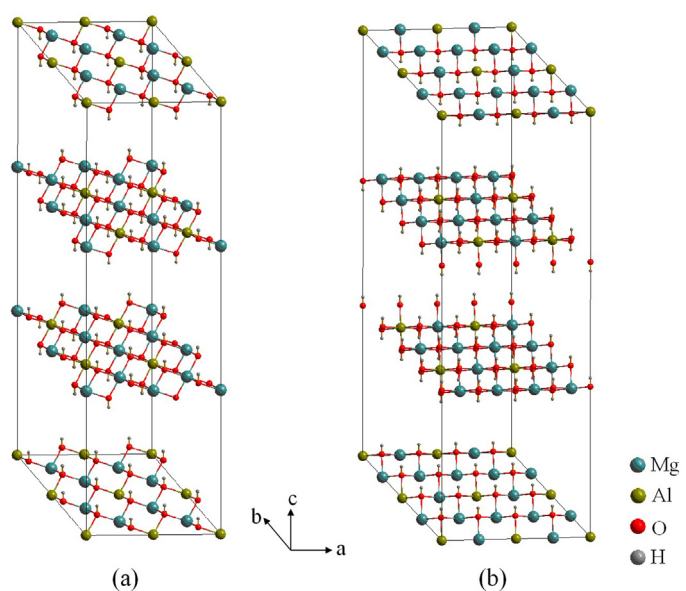


Fig. 1. Sub-lattices of MgAl-LDHs with Mg/Al ratio of two (a) and three (b).

[1,42,43]. The typical structure is the $\text{Mg}^{2+}/\text{Al}^{3+} = 2$ and 3 with $R-3m$ space-group [6], of which the Al^{3+} exists with highly dispersed form. Both two structures are three laminates as a repeating unit, shown in Fig. 1. The previous study [44] shows that the intercalated CO_3^{2-} anions could affect the original space-group for LDH structure, if the symmetry of the incoming anions matches the local symmetry of the interlayer site (D_{3h} or O_h). However, it needs to meet two conditions in order to maintain the same space group after introduction of CO_3^{2-} group: the plane containing the four atoms of CO_3^{2-} need to parallel to the layer of LDH and CO_3^{2-} group need to be in the middle of the triangular pyramid-shaped (as shown in Fig. 2, the four vertices of the triangular pyramid as Al^{3+} , and three of which as an equilateral triangle in a lamellae). Accordingly, the CO_3^{2-} group has two spatial orientations in the interlayer as shown in Fig. 2(I) and (II). The calculation results indicate that the structure (II) is less stable and most likely becomes the type (I). The models of ZnCr-LDHs with CO_3^{2-} in the interlayer are obtained as the same approach.

All calculations are performed with the DFT method using Dmol3 [45,46] module in Material Studio software package [47]. The initial configuration is fully optimized by using Perdew–Wang (PW91) [48] generalized gradient approximation (GGA) method with the double numerical basis sets plus polarization function

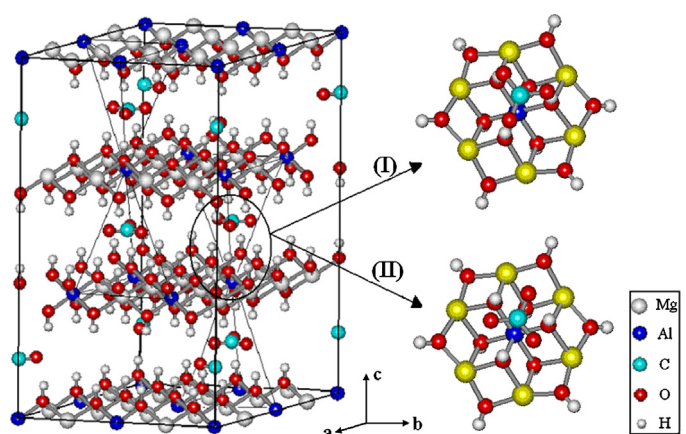


Fig. 2. Crystal structure of MgAl-LDHs (Mg/Al ratio of three) with CO_3^{2-} in the interlayer.

(DNP). The core electrons for metals are treated by effective core potentials (ECP). The converged criterion of SCF is within 1.0×10^{-5} hartree/atom and the converged criterion of structure optimization 5.0×10^{-3} hartree/bohr. The Brillouin zone is sampled by $1 \times 1 \times 1$ k -points, considering such a large supercell LDH system, and the testing calculation results reveal that increasing the k -points does not affect the results.

2.2. Synthesis of LDH samples

All the LDH samples were synthesized by a coprecipitation method in low supersaturating condition at room temperature [49]. For the synthesis of MgAl-LDHs, a mixture of $\text{Mg}(\text{NO}_3)_2 \cdot 6\text{H}_2\text{O}$ and $\text{Al}(\text{NO}_3)_3 \cdot 9\text{H}_2\text{O}$ with $\text{Mg}^{2+}/\text{Al}^{3+}$ molar ratio 2 was dissolved in 100 mL of deionized water to give solution A ($[\text{Mg}^{2+}] + [\text{Al}^{3+}] = 1.2 \text{ M}$). NaOH and Na_2CO_3 were dissolved in 100 mL of deionized water to give a mixed base solution B. The concentration of the base was related to those of the metal ions in solution A as follows: $[\text{CO}_3^{2-}] = 2.0 [\text{Al}^{3+}]$, $[\text{OH}^-] = 1.6 ([\text{Mg}^{2+}] + [\text{Al}^{3+}])$. Solution A and B were simultaneously added drop wise to a four-necked flask containing 50 mL of deionized water at room temperature. The pH value was held constant at 10.0. The resulting suspension was further aged at 60°C for 24 h with stirring. The procedures for ZnCr-LDHs with $\text{Zn}^{2+}/\text{Cr}^{3+}$ molar ratio 2 were similar with that of MgAl-LDHs. The starting salts used were $\text{Zn}(\text{NO}_3)_2 \cdot 6\text{H}_2\text{O}$ and $\text{Cr}(\text{NO}_3)_3 \cdot 9\text{H}_2\text{O}$.

2.3. Characterization

XRD were collected on a Shimadzu XRD-6000 diffractometer under the following conditions: 40 kV, 30 mA, graphite-filtered $\text{Cu K}\alpha$ radiation ($\lambda = 0.15418 \text{ nm}$). The powder samples were step-scanned in steps of 0.04° (2θ) using a count time of 10 s/step. FT-IR spectra were recorded in the range of $400\text{--}4000 \text{ cm}^{-1}$ with 2 cm^{-1} resolution on a Bruker Vector-22 Fourier transform spectrometer using KBr pellet technique (1 mg of sample in 100 mg of KBr). The specific surface area determination and pore volume and size analysis were performed by BET and BJH methods, with nitrogen adsorption at 77 K using a Quantachrome Autosorb-1C-VP Analyzer. Prior to the measurements, the samples were degassed at 80°C for 6 h. UV-vis diffuse reflectance spectra were recorded at room temperature in air by means of a Shimadzu UV-2501PC spectrometer equipped with an integrating sphere attachment using BaSO_4 as background. Elemental analyses for metals in the LDH samples were performed with a Shimadzu ICP-ES on solutions prepared by dissolving the samples in dilute HCl. Zeta potential measurements were carried out on a Malvern ZETASIZER 3000HS analyzer.

2.4. Elimination of pollutants from solution

Photocatalytic capabilities of MgAl- and ZnCr-LDHs were evaluated using the photodegradation of MB, MO or formaldehyde under visible light irradiation as model reactions. A quartz beaker (capacity 150 mL) was used as the photoreaction vessel. Typically, the reaction system containing MB or MO ($1 \times 10^{-5} \text{ M}$, 100 mL) and LDH sample (0.3 g/L) was magnetically stirred in the dark for 240 min. Then a new reaction system was exposed to light from a 300 W Xe lamp equipped with a UV cutoff filter ($\lambda \geq 420 \text{ nm}$) for 240 min. At specific time intervals, 3 mL of the reaction solution was withdrawn by a syringe. The solution was centrifuged to remove the catalyst sample before being analyzed by UV-vis adsorption spectroscopy using a Shimadzu UV-2501PC spectrophotometer. Blank reaction was carried out by following the same procedure without adding of LDH. For the elimination

of formaldehyde, the procedures were the same, excepting for using acetylacetone spectrophotometric method before being analyzed.

3. Results and discussion

3.1. DFT calculation for band structure of LDH samples

According to the fundamental processes of the semiconductor photocatalytic reaction and the thermodynamics about the transfer reaction of the excited electrons [27,28], the photocatalytic activity of the semiconductor material is closely related with its structural characters of the band gap (including the band gap energy (E_g), band structure and the electric potential of both CB and VB). To better understand the electronic band structure of both MgAl- and ZnCr-LDHs, periodic DFT calculation is performed to calculate the total and partial electronic density of states (TDOS and PDOS) and the results are shown in Fig. 3. Although the bandgap from the DFT calculations is usually underestimated, they could provide further insight into the investigated materials [50,51]. The composition of electronic band structure could be analyzed by the density of states (DOS), and the bottoms of conduction band and the tops of valence band could be clarified [52,53]. The calculation results reveal that, for the Mg_xAl -LDHs (molar ratio $x = 2$ and 3), the top of the VB and the bottom of the CB are mainly dominated by the 3s of Mg, 2p of O, and 3p of Al. The p orbital from the LDH layers contribute to the TDOS, with the band gap of 5.63 and 7.41 eV for Mg_2Al - and Mg_3Al -LDHs, respectively, while, for the Zn_xCr -LDHs the O 2p and Zn (Cr) 3d orbital from the LDH layers contribute to the TDOS, with the band gap of 2.50 and 2.80 eV for Zn_2Cr - and Zn_3Cr -LDHs, respectively. The result is close to the reported experiment value 2.2 eV for Zn_2Cr -LDHs sample [41]. For both Mg_xAl - and Zn_xCr -LDHs, the energy gap becomes larger as the x value increases. It is interesting to note that when the x value increases (i.e., the percentage content of M^{3+} in the main layers decrease), s and p electron density decreases. Therefore, the delocalization for the electrons of CB is weakened, that may lead to the energy gap larger directly. In addition, the number of the interlayer CO_3^{2-} groups decrease as the increase of the x value, and the VB near the Fermi level of the 2p electron peak also appears the same changes. Meanwhile, recent investigations employing the combined ^1H and ^{25}Mg MAS NMR technique have revealed that distribution of the Mg and Al atoms on LDH layer is not random [54]. And, in the structure of ZnCr-LDHs, Cr cations are surrounded by six Zn cations, which are disclosed by using EXAFS and UV-vis techniques [55]. From the point of view of LDH structure, the coefficient x could not change the intrinsic properties of LDH sample. Therefore, in the following experiment work, two samples of ZnCr- and MgAl-LDHs with $\text{M}^{2+}/\text{M}^{3+}$ molar ratio 2 are prepared and used as the photocatalysts in the experimental work.

The elimination tests of organic pollutants (MB, MO or formaldehyde) from solution using Mg_2Al - and Zn_2Cr -LDHs are carried out in the dark place with the similar condition of the processes under visible light irradiation. Both MB and MO are common dyes to test the photocatalytic activity. The original MB solution is weak alkaline (~ 7.8), while MO is weak acid (~ 6.7). However, with consideration of the photosensitization effect by organic dyes (MB and MO), it is inadequate to evaluate the really photocatalytic activity of the pristine LDH through the elimination test of MB or MO. Herein, formaldehyde, MB and MO solution are applied in the photocatalytic test. The use of formaldehyde as a probe molecule has several merits: it has no visible light absorption and the photodegraded reaction is relative simple [36]. The experimental results would compare and discuss with the DFT calculation.

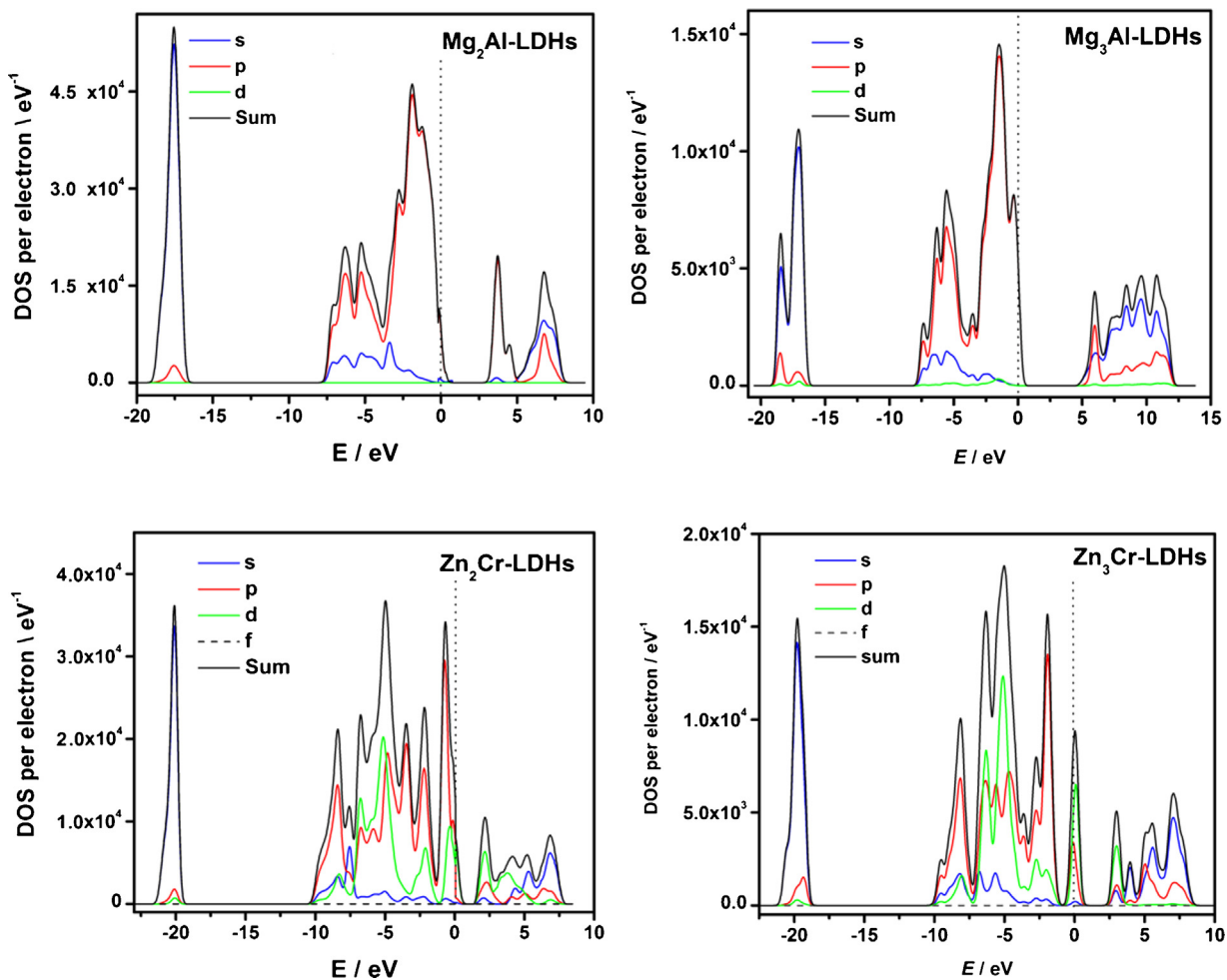


Fig. 3. Total and partial electronic density of states (TDOS and PDOS) for the different LDH samples. The Fermi energy level E_F was set to zero.

3.2. Catalyst characterization

The XRD patterns of the as-prepared Mg₂Al- and Zn₂Cr-LDHs (Fig. 4) exhibit the characteristic diffraction peaks of well-crystallized LDH material with a series of (001) harmonics at low angle [9,56]. Assuming a hexagonal lattice with $R-3m$ rhombohedral symmetry, the lattice parameters c (= d_{003}) and a (= d_{110}) are calculated and listed in Table 1. The unit cell parameter a is the average distance between two metal ions in the layers and

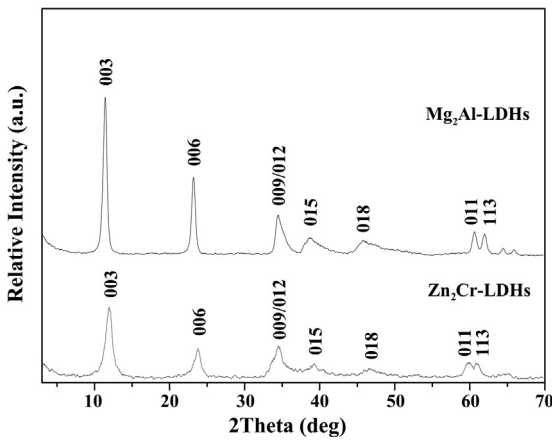


Fig. 4. XRD patterns of MgAl- and ZnCr-LDHs with M^{2+}/M^{3+} molar ratio 2.

c being 3 times the distance from the center of one layer to the next [9]. Meanwhile, the average crystal size of LDH is calculated using Scherrer equation (Table 1). The textural analyses for both LDH samples are done and the surface area values are also included in Table 1.

The FT-IR spectra of MgAl- and ZnCr-LDHs in the region of 400–4000 cm⁻¹ (Fig. 5) show typical adsorption peaks of hydrotalcite phase with CO_3^{2-} as counteranion [57]. The strong and broad adsorption band observed around 3400 cm⁻¹ is associated with a superposition of the hydroxyl stretching band $\nu(OH_{str})$ arising from metal-hydroxyl groups and hydrogen-bonded interlayer water molecules. Another adsorption band corresponding to water deformation, $\delta(H_2O)$, is recorded around 1635 cm⁻¹. The intense adsorption band at 1384 cm⁻¹ is ascribed to the ν_3 (asymmetric stretching) mode of CO_3^{2-} ions. The other bands observed in the low frequency 500–800 cm⁻¹ region are interpreted as the vibration modes of metal-oxygen (M–O) and metal-hydroxyl (M–OH) groups in the lattices [58].

Table 1
Unit cell parameters, crystallite sizes, and surface areas of LDH samples.

Samples	Unit cell parameter (nm)		Crystal size (nm)		S_{BET} (m ² g ⁻¹)
	c value	a value	D_{003}	D_{110}	
Mg ₂ Al-LDHs	2.27	3.02	11.9	16.8	42.3
Zn ₂ Cr-LDHs	2.25	3.07	10.1	10.0	48.9

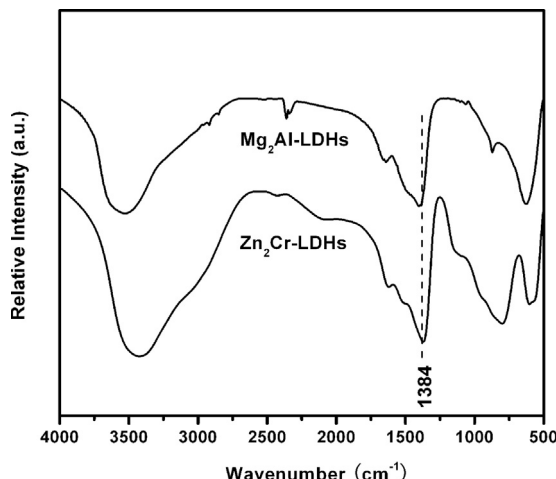


Fig. 5. FT-IR spectra of Mg_2Al - and Zn_2Cr -LDHs.

The UV-vis spectrum is believed to be a powerful tool to provide important information about the optical properties of the photocatalytic material. For Mg_2Al -LDHs (Fig. 6), no obvious adsorption peaks could be observed in the whole visible light region (400–800 nm), indicating that such MgAl -LDHs sample is inert with the irradiation of visible light. Zn_2Cr -LDHs sample exhibits a similar adsorption behavior and two maxima in the visible region at ~ 405 nm and ~ 565 nm could be observed (Fig. 6), which is similar with the reported UV-vis spectra data for Zn_2Cr -LDHs (visible region at 410 nm and 570 nm) [55]. Our recent investigations show that [32] the photocatalytic sample (the supported TiO_2) exhibited the absorption in visible region, but there is no photocatalytic activity under visible light irradiation for the degradation of formaldehyde and dye sensitization plays an important role in degradation of MB under visible light irradiation. In order to confirm the relationship between the removal ability for contaminants and the optical properties of LDH material, the MB, MO and formaldehyde are chosen as target contaminants and the elimination tests are carried out.

3.3. Removal of organic pollutants from solution with LDH samples

Any change in the concentration of formaldehyde in the solution is observed when the solution is put in contact with LDH samples

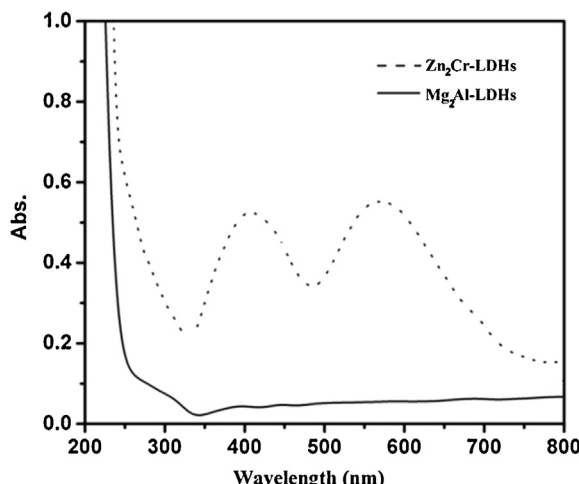


Fig. 6. UV-vis adsorption spectra of Mg_2Al - and Zn_2Cr -LDHs.

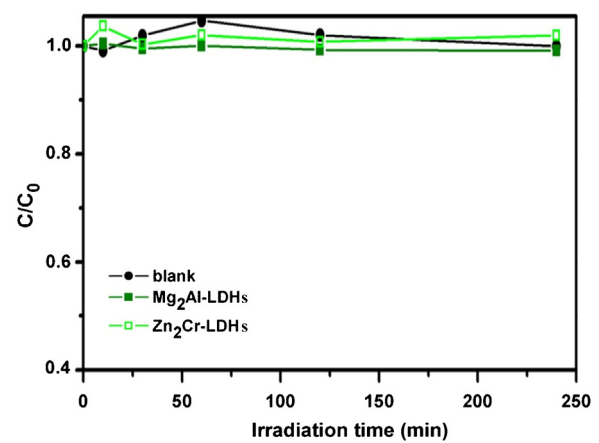


Fig. 7. The normalized concentration change of formaldehyde solution with or without LDH samples.

during the 240 min irradiation time (Fig. 7). The concentration of formaldehyde is almost no change during the reaction time under the visible light. The results show that both LDH samples have no photocatalytic activity on removal of formaldehyde. Fig. 8 shows the concentration change of MB and MO solution versus irradiation time with and without LDH samples. The removal efficiency of MB without LDH is only 10% after 240 min visible light irradiation. With the addition of Zn_2Cr -LDHs, the removal efficiency is still relatively low, about 4% in the dark and 21% in the visible light. However, it is unexpected to find that, the removal efficiency of MB is apparently increased to 35% with the existence of Mg_2Al -LDHs. Further investigations on the removal of acid dye (MO) are carried out with both LDH samples. Almost no decreasing of the concentration of MO could be observed without LDH material under the visible light. Unlike the results of the removal of MB, whether in the dark or visible light, a much stronger removal of MO is observed for Zn_2Cr -LDHs, and the removal efficiency reaches 76%. However, for the Mg_2Al -LDHs, the removal efficiency is only about 9% without light and 13% with the visible light irradiation. To better know the degradation activity, the final removal results should exclude the amount of the blank and adsorption in the dark (Table 2).

3.4. Photocatalytic performance elucidation

Photocatalytic processes are widely thought to be based on the generation of electron and hole pairs by means of light radiation. It could be concluded from the experimental work that the Mg_2Al -LDHs and Zn_2Cr -LDHs have no photocatalytic activity for the removal formaldehyde, and for the removal dye (MB and MO), two types of LDH samples show the low photocatalytic activity (Table 2). However, Silva et al. [38] reported that ZnCr -LDHs is very active for the photocatalytic oxidation of water by visible light with AgNO_3 solution dispersed in the reaction cell. The major difference with the Silva's work is the addition of AgNO_3 solution. The AgNO_3 is widely adopted as sacrificial electron acceptor and the formation of Ag nanoparticles during the photocatalytic reaction would enhance the electron/hole separation [27,59,60]. By the way, in the XRD pattern reported by Silva et al. (Fig. 2 in Ref. [38]), formation of amorphous metal oxide may be existence, as evidenced by the broad diffraction peak from the $2\theta = 34\text{--}64^\circ$. In this study, the pristine ZnCr -LDHs is prepared and used in testing the photocatalytic activity. Combined the analysis of DOS and structure of LDH, the outermost surface of LDH material is constituted by the hydroxyl groups. The hydroxyl groups have low contribution to the bottoms of conduction band and the tops of valence band, which would hinder the photoinduced electrons or holes transfer to the scavengers.

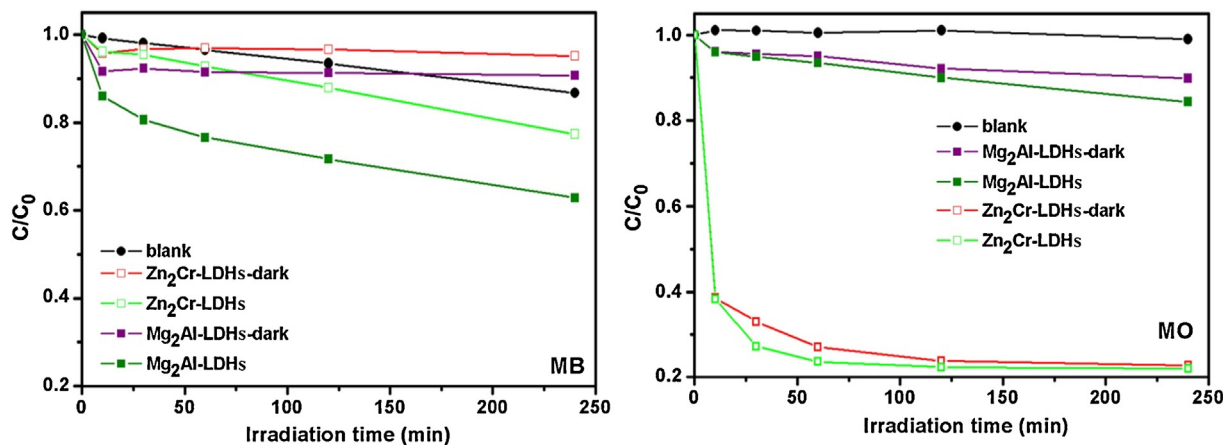


Fig. 8. The normalized concentration change of MB and MO solution versus irradiation time with Zn₂Cr- and Mg₂Al-LDHs under different irradiation condition.

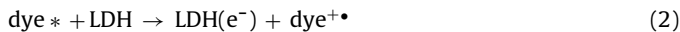
Table 2

Comparison of the removal results of MB and MO under dark condition or visible light irradiation with different LDH samples.

		Irradiation time	Blank	Under dark	Under light	Photoassisted degradation
MB	Mg ₂ Al-LDHs	240 min	10%	8%	35%	17%
	Zn ₂ Cr-LDHs	240 min	10%	3%	21%	8%
MO	Mg ₂ Al-LDHs	240 min	0%	10%	14%	4%
	Zn ₂ Cr-LDHs	240 min	0%	76%	76%	0%

If excess electrons and holes remain on the semiconductor, then subsequent electron–hole charge separation is likely to be very inefficient due to rapid reaction of recombination processes.

Zhao et al. [61–64] reported that dyes could be photodegraded under visible light with TiO₂, the initial degradation step is different from the one under UV light illumination in the presence of the semiconductor. The excited dye injects an electron to the conduction band of semiconductor, whence it is scavenged by preadsorbed oxygen to form active oxygen radicals similar to those in UV irradiation processes. Combined the experiment results of removal organic dyes and DFT calculation results, it indicate that the processes of photodegradation dye (MB and MO) on LDH could be self-sensitized photodegradation pathways. This reaction mechanism would be similar to the mechanism reported by Zhao's group previously. The photodegradation processes of dye are proposed as shown in the following steps:



For the organic dye molecules, irradiation by the visible light is the initial step for the photodegradation steps. However, formaldehyde could not be photoexcited by the visible light, which may hinder the occurrence of the subsequent steps. Our experimental results demonstrate that both Mg₂Al-LDHs and Zn₂Cr-LDHs show no photocatalytic activity for removal of formaldehyde under the visible light (Fig. 7). However, the MO and MB could absorb photons to form photoexcited dye which could inject the electron into the CB of LDH, and two types of LDH samples show photocatalytic activity under visible light irradiation. In summary, the experimental

and theoretical results indicate the removal processes of pollutants molecules are carried out over LDH materials through photoassisted degradation and adsorption processes other than intrinsic photocatalytic processes as a result of the textual characters of LDH.

To further elucidate effect of O₂ on photoassisted degradation processes, the excessive O₂ is added in the reaction system during the photodegradation reaction. Because removal behavior of MO with Mg₂Al-LDHs and Zn₂Cr-LDHs is almost same with or without light irradiation, the influence of O₂ on photocatalytic degradation of MB is performed and provided in Fig. 9. The removal efficiency of MB without LDH is 51% after 240 min visible light irradiation. With the addition of Zn₂Cr-LDHs and Mg₂Al-LDHs, the removal efficiency is 65% and 86%, respectively. Compared with the degradation curve without the added excessive O₂ (Fig. 8), both Zn₂Cr-LDHs and Mg₂Al-LDHs exhibit a better photocatalytic performance. The results indicate that the O₂ play an important role in photoassisted degradation processes under visible light.

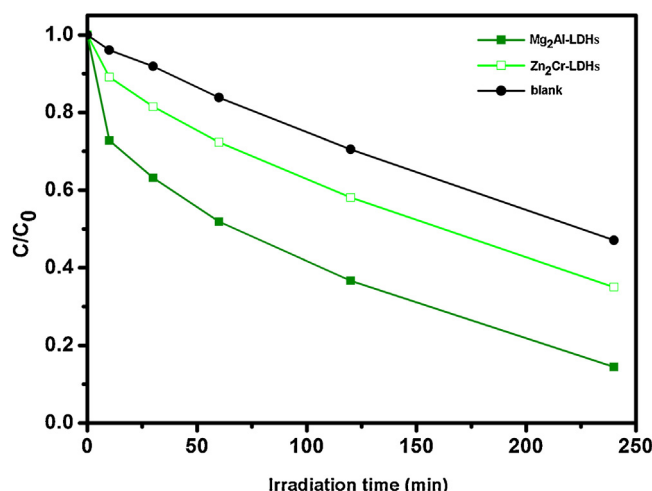


Fig. 9. The effect of O₂ on photocatalytic degradation of MB solution with Zn₂Cr- and Mg₂Al-LDHs under visible light condition.

Meanwhile, from the above analyses of DOS study, it is known that the CB of Mg_2Al -LDHs is mainly dominated by the 3s of Mg, 2p of O, and 3p of Al, and the O 2p and Zn (Cr) 3d orbitals from the Zn_2Cr -LDHs layers contribute to the TDOS below and above CB. However, from the point of view of the LDH structure, the outermost surface of LDH material is constituted by the hydroxyl groups, which inhibit the photoexcited dye to contact the LDH layer. Therefore, the photoexcited dye would be difficult to inject electron to the CB of LDH, which would hinder the photoassisted processes and lead to decrease the photoassisted efficiency. By contrast, the photoassisted processes would be much easier to carry out on the TiO_2 surface, because the Ti 3d states govern the CB of TiO_2 and the surface of TiO_2 are constituted by the atoms of Ti and O [39]. The reported experimental results have examined the TiO_2 -assisted photodegradation under visible light [32,62–64].

For the adsorption performances with different dyes and types of LDH, the CO_3^{2-} in the interlayer of pristine LDH material is considered. It is revealed that organic dye molecules are difficult to displace the interlaminar CO_3^{2-} through anion-exchange reaction [16]. Therefore, the adsorption of MB or MO molecules could be attributed to the surface adsorption. According to the literatures, the surface adsorption involves the adhesion of the target molecules to the surface of LDH, and thus allowing the formation of a molecular or atomic film [61]. Hence, the difference in adsorption capability of Mg_2Al - and Zn_2Cr -LDHs in our case is closely related with the surface area and the surface states of such particles of LDH in the solution during the adsorption process. It is shown that Mg_2Al - and Zn_2Cr -LDHs exhibit different adsorption capability in MB and MO solution (Fig. 8): that is, Mg_2Al -LDHs sample has the much higher adsorption ability for the removal of MB molecules in the solution; however, for the removal of MO, Zn_2Cr -LDHs sample is better. According to the results of the N_2 adsorption characterization in Table 1, the surface area of both LDH samples is very similar. Therefore, the different adsorption capability of Mg_2Al - and Zn_2Cr -LDHs in MB or MO solution might be ascribed to the surface states of particles of LDH in the solution. Considering the pH value of the original MB and MO solution, the isoelectric point of Mg_2Al - and Zn_2Cr -LDHs are tested by Zeta potential measurement and the results are 7.59 and 6.88, respectively. In general, the isoelectric point values at pH 7.59 of Mg_2Al -LDHs are weak alkaline and very close to the pH value of the original MB solutions (~7.8). While, for Zn_2Cr -LDHs sample, the weak acid isoelectric point values at pH 6.88 are close to the pH value of the original MO solutions (~6.7). According to the Gouy–Chapman–Stern model [65], the thickness of the electrical double layer is slightly, and the LDH colloidal solids in the solution are instable under the pH value of isoelectric point. Therefore, for the solution containing MB molecules, the electrostatic attraction between MB molecules and Mg_2Al -LDHs colloidal solids is much stronger than Zn_2Cr -LDHs, and the adsorption capacity of MB molecules on Mg_2Al -LDHs colloidal solids increases consequently. Likewise, the stronger electrostatic attraction between Zn_2Cr -LDHs particles and the MO molecules leads to the higher elimination results for MO.

4. Conclusions

In this paper, typical Mg_2Al - and Zn_2Cr -LDHs are prepared and used to discuss the essence of elimination of organic pollutants from water solution. For the Mg_2Al -LDHs, DFT calculation and UV-vis spectra experimental results show that no electron–hole pairs could be generated under the irradiation of visible light due to the large calculated gap energy above 5.00 eV, whereas Zn_2Cr -LDHs could be thought of a semiconductor material and is sensitive to the irradiation of visible light. Nevertheless, the rapid charge recombination and low efficiency in electron/hole separation may result in the limited photocatalytic activity. In the experimental work,

both Mg_2Al - and Zn_2Cr -LDHs show no photocatalytic activity for the removal of formaldehyde molecules, and the elimination processes of organic dyes (MB and MO) in the solution are proposed to be carried out through the photoassisted degradation and surface adsorption processes rather than the photocatalysis manner. Moreover, the different adsorption capability of Mg_2Al - and Zn_2Cr -LDHs for the both dye molecules could be attributed to the different isoelectric points of LDH material.

Acknowledgements

We acknowledge generous financial support from the National Natural Science Foundation of China, the 973 Program (No. 2011CBA00506). This paper is also supported by the “Chemical Grid Project” of Beijing University of Chemical Technology.

References

- [1] C. Grégorio, Bioresource Technology 97 (2006) 1061–1085.
- [2] B. Özkaya, Journal of Hazardous Materials B 129 (2006) 158–163.
- [3] O. Ozdemir, B. Armagan, M. Turan, M.S. Celik, Dyes Pigments 62 (2004) 49–60.
- [4] K.H. Goh, T.T. Lim, Z.L. Dong, Water Research 42 (2008) 1343–1368.
- [5] F. Figueras, Topics in Catalysis 29 (2004) 189–196.
- [6] F. Cavaní, F. Trifirò, A. Vaccari, Catalysis Today 11 (1991) 173–301.
- [7] V. Rives, Layered Double Hydroxides: Present and Future, 1st ed., Nova Sci. Pub., New York, 2001 (Chapter 1).
- [8] S.M. Auerbach, in: K.A. Carrado, P.K. Dutta (Eds.), Handbook of Layered Materials, M. Dekker Inc., New York, 2004.
- [9] F. Millange, R.I. Walton, D. O'Hare, Journal of Materials Chemistry 10 (2000) 1713–1720.
- [10] M. Cantu, E. Lopez-Salinas, J.S. Valente, R. Montiel, Environmental Science and Technology 39 (2005) 9715–9720.
- [11] P.C. Panan, G.A. Gomes, J.B. Valim, Microporous and Mesoporous Materials 21 (1998) 659–665.
- [12] J. Orthman, H.Y. Zhu, G.Q. Lu, Separation and Purification Technology 31 (2003) 53–59.
- [13] L.P. Cardoso, J.B. Valim, Journal of Physics and Chemistry of Solids 67 (2006) 987–993.
- [14] A. Legrouri, M. Lakraimi, A. Barroug, A. De Roy, J.P. Besse, Water Research 39 (2005) 3441–3448.
- [15] Y.W. You, H.T. Zhao, G.F. Vance, Applied Clay Science 21 (2002) 217–226.
- [16] F. Li, X. Duan, Structure and Bonding 119 (2006) 193–223.
- [17] S.N. Frank, A.J. Bard, Journal of the American Chemical Society 97 (1975) 7427–7433.
- [18] A.L. Linsebigler, G.Q. Lu, J.T. Yates, Chemical Reviews 95 (1995) 735–758.
- [19] B. Ohtani, Y. Ogawa, S. Nishimoto, Journal of Physical Chemistry B 101 (1997) 3746–3752.
- [20] L.J. Yang, S.J. An, W.I. Park, G.C. Yi, W. Choi, Advanced Materials 16 (2004) 1661–1664.
- [21] O. Seven, B. Dindar, S. Aydemir, D. Metin, M.A. Ozinel, S. Icli, Journal of Photochemistry and Photobiology A 165 (2004) 103–107.
- [22] A. McLaren, T. Valdes-Solis, G.Q. Li, S.C. Tsang, Journal of the American Chemical Society 131 (2009) 12540–12541.
- [23] F. Lu, W.P. Cai, Y.G. Zhang, Advanced Functional Materials 18 (2008) 1047–1056.
- [24] X. Xu, R.J. Lu, X.F. Zhao, Y. Zhu, S.L. Xu, F.Z. Zhang, Applied Catalysis B: Environmental 125 (2012) 11–20.
- [25] R. Baron, C.H. Huang, D.M. Bassani, A. Onopriyenko, M. Zayats, I. Willner, Angewandte Chemie International Edition 44 (2005) 4010–4015.
- [26] X. Zong, H.J. Yan, G.P. Wu, G.J. Ma, F.Y. Wen, L. Wang, C. Li, Journal of the American Chemical Society 130 (2008) 7176–7177.
- [27] H.J. Zhang, G.H. Chen, D.W. Bahnemann, Journal of Materials Chemistry 19 (2009) 5089–5121.
- [28] M.R. Hoffmann, S.T. Martin, W.Y. Choi, D.W. Bahnemann, Chemical Reviews 95 (1995) 69–96.
- [29] D.G. Evans, R.C.T. Slade, in: D.M.P. Mingos (Ed.), Structure and Bonding (Berlin), vol. 119, Springer, New York, 2005, pp. 4–11.
- [30] X.F. Zhao, L. Wang, X. Xu, X.D. Lei, S.L. Xu, F.Z. Zhang, AIChE Journal 58 (2012) 573–582.
- [31] Y.F. Zhao, M. Wei, J. Lu, Z.L. Wang, X. Duan, ACS Nano 3 (2009) 4009–4016.
- [32] R.J. Lu, X. Xu, J.P. Chang, Y. Zhu, S.L. Xu, F.Z. Zhang, Applied Catalysis B: Environmental 111 (2012) 389–396.
- [33] A. Mantilla, F. Tzompantzi, J.L. Fernández, J.A.I. Díaz Gógora, G. Mendoza, R. Gómez, Catalysis Today 148 (2009) 119–123.
- [34] A. Mantilla, G.J. Acatitl, G.M. Mendoza, F. Tzompantzi, R. Gómez, Industrial and Engineering Chemistry Research 50 (2011) 2762–2767.
- [35] M. Shao, J. Han, M. Wei, D. Evans, X. Duan, Chemical Engineering Journal 168 (2011) 519–524.
- [36] X. Yan, T. Ohno, K. Nishijima, R. Abe, B. Ohtani, Chemical Physics Letters 429 (2006) 606–610.
- [37] J.S. Valente, F. Tzompantzi, J. Prince, J.G.H. Cortez, R. Gomez, Applied Catalysis B: Environmental 90 (2009) 330–338.

[38] C.G. Silva, Y. Bouizi, V. Fornés, H. García, *Journal of the American Chemical Society* 131 (2009) 13833–13839.

[39] J.L. Gunjakar, T.W. Kim, H.N. Kim, I.Y. Kim, S.J. Hwang, *Journal of the American Chemical Society* 133 (2011) 14998–15007.

[40] X. Chen, L. Liu, P.Y. Yu, S.S. Mao, *Science* 331 (2011) 746–750.

[41] R. Long, N.J. English, *Physical Chemistry Chemical Physics* 13 (2011) 13698–13703.

[42] H. Yan, M. Wei, J. Ma, D.G. Evans, X. Duan, *Journal of Physical Chemistry A* 114 (2010) 7369–7376.

[43] M. Pu, Y.L. Wang, L.Y. Liu, Y.H. Liu, J. He, D.G. Evans, *Journal of Physics and Chemistry of Solids* 69 (2008) 1066–1069.

[44] A.V. Radha, P.V. Kamath, C. Shivakumara, *Journal of Physical Chemistry B* 111 (2007) 3411–3418.

[45] B. Delley, *Journal of Chemical Physics* 92 (1990) 508.

[46] B. Delley, *Journal of Chemical Physics* 113 (2000) 7756.

[47] Dmol3 Module, MS Modeling, Version 5.5, Accelrys Inc., San Diego, CA, 2003.

[48] J.P. Perdew, J.A. Chevary, S.H. Vosko, K.A. Jackson, M.R. Pederson, D.J. Singh, C. Fiolhais, *Physical Review B* 46 (1992) 6671–6687.

[49] K.K. Rao, M. Gravelle, J.S. Valente, F. Figueras, *Journal of Catalysis* 173 (1998) 115–121.

[50] Z. Yi, J. Ye, N. Kikugawa, T. Kako, S. Ouyang, H. Stuart-Williams, H. Yang, J. Cao, W. Luo, Z. Li, Y. Liu, R.L. Withers, *Nature Materials* 9 (2010) 559–564.

[51] J. Tang, Z. Zou, J. Ye, *Journal of Physical Chemistry C* 111 (2007) 12779–12785.

[52] H. Yu, H. Irie, K. Hashimoto, *Journal of the American Chemical Society* 132 (2010) 6898–6899.

[53] J. Sato, H. Kobayashi, Y. Inoue, *Journal of Physical Chemistry B* 107 (2003) 7970–7975.

[54] P.J. Sideris, U.G. Nielsen, Z. Gan, C.P. Grey, *Science* 321 (2008) 113–117.

[55] H. Rousset, V. Briois, E. Elkaim, A. Roy, J.P. Besse, J.P. Jolivet, *Chemistry of Materials* 13 (2001) 329–337.

[56] C. Busetto, G. Del Piero, G. Mamara, F. Trifiró, A. Vaccari, *Journal of Catalysis* 85 (1984) 260–266.

[57] M.J. Hernandez-Moreno, M.A. Ulibarri, J.L. Rendon, *Physics and Chemistry of Minerals* 12 (1985) 34–38.

[58] M.K. Titulaer, J.B.H. Jansen, J.W. Geus, *Clays and Clay Minerals* 42 (1994) 249–258.

[59] A. Wood, M. Giersig, P. Mulvaney, *Journal of Physical Chemistry B* 105 (2001) 8810–8815.

[60] V. Subramanian, E.E. Wolf, P.V. Kamat, *Journal of the American Chemical Society* 126 (2004) 4943–4950.

[61] F. Zhang, J. Zhao, T. Shen, H. Hidaka, E. Pelizzetti, N. Serrpone, *Applied Catalysis B: Environmental* 15 (1998) 147–156.

[62] T. Wu, T. Lin, J. Zhao, H. Hidaka, N. Serrpone, *Environmental Science and Technology* 33 (1999) 1379–1387.

[63] J. Zhao, T. Wu, K. Wu, K. Oikawa, H. Hidaka, N. Serrpone, *Environmental Science and Technology* 32 (1998) 2394–2400.

[64] C. Chen, W. Zhao, J. Li, J. Zhao, *Environmental Science and Technology* 36 (2002) 3604–3611.

[65] K.Y. Foo, B.H. Hameed, *Journal of Hazardous Materials* 170 (2009) 552–559.